

Penetrative turbulence associated with mesoscale surface heat flux variations

Jahrul M Alam* and M Alamgir Hossain
Department of Mathematics and Statistics
Memorial University, Canada

Abstract

This article investigates penetrative turbulence in the atmospheric boundary layer. Using a large eddy simulation approach, we study characteristics of the mixed layer with respect to surface heat flux variations in the range from 231.48 Wm^{-2} to 925.92 Wm^{-2} , and observe that the surface heterogeneity on a spatial scale of 20 km leads to downscale turbulent kinetic energy cascade. Coherent fluctuations of mesoscale horizontal wind is observed at 100 m above the ground. Such a surface induced temporal oscillations in the horizontal wind suggest a rapid jump in mesoscale wind forecasts, which is difficult to parameterize using traditional one-dimensional ensemble-mean models. Although the present work is idealized at a typical scale (20 km) of surface heterogeneity, the results help develop effective subgrid scale parameterization schemes for classical weather forecasting mesoscale models.

1 Introduction

Earth's surface is assumed to play a distinctive influence in weather and climate systems (Stull, 1976). The surface influence generates horizontal convection as a result of differential heating along one horizontal boundary of the atmospheric boundary layer (ABL) (Lane, 2008; Scotti and White, 2011). Coherent mesoscale motions are reported by many studies, where the effect of surface heterogeneity are investigated numerically on scales of few hundred kilometers, using a grid spac-

ing of $\Delta x \sim \mathcal{O}(10 \text{ km})$ (Skamarock and Klemp, 2008; Lin, 2007). However, in the geophysical fluid dynamics community, controversial opinions exist on whether horizontal convection due to differential heating at the same level would lead to turbulence, or drive large scale overturning circulations (Paparella and Young, 2002; Scotti and White, 2011). A century old experimental result by Sandström (1908) leads to the opinion that a sustained circulation cannot occur if the level of the heating source is the same as that of the cooling source. This hypothesis is supported theoretically by the anti-turbulence theorem of Paparella and Young (2002). However, Scotti and White (2011) employed a direct numerical simulation of horizontal convection at Rayleigh number 10^{10} to show that a flow driven by the horizontal convection exhibits the characteristics of a true turbulent flow. Clearly, some fundamental aspects of solar heating at the earth's surface is not fully understood.

Much of our current understanding of surface induced phenomena depends on numerical simulations and measurements/observations. For example, lightning data over Houston, USA between years of 1989 and 2000 indicates that highest flash densities occur over urban areas. Measurements of turbulence for the 43 years period from 1958 to 2001 in the North Atlantic, USA, and European sectors conclude that clear-air turbulence increases in these regions by 40 – 90% as a result of the urban induced impact on vertical transport and mixing of penetrative ABL turbulence. Note that the average horizontal flux of kinetic energy at a height $\sim 100 \text{ m}$ from the ground is about 1000 W m^{-2} . A destabilization of this huge energy flux due to differential heating on the surface may cause catastrophic impact on the tur-

*Corresponding author's email: alamj@mun.ca

bulent atmosphere. Since penetrative turbulence in the atmosphere (see Stull, 1976) is primarily characterized by solar heating, perturbations to boundary layer structures by human activities (*e.g.* urbanization) are sensitive to vertical mixing and transport (Bryan and Fritsch, 2002; Lane, 2008).

This article reports on a large eddy simulation (LES) based numerical model in order to characterize penetrative turbulence over heterogeneous land surface. Primary objectives of this short article includes the investigation of evidences whether horizontal convection transports large quantities of heat, as well as sustains large amounts of diapycnal mixing with a relatively small amount of dissipation. We demonstrate that differential surface heating on scales of a typical modern city cascades kinetic energy downscale, which – in the absence of shear – is sufficient to initiate a turbulent flow. The computational fluid dynamics approach used in this work is fully detailed by Alam et al. (2014). This method filters the governing equations using a multiresolution approach, and employs a Smagorinsky type eddy viscosity model for the subfilter scale processes. We use a sixth order weighted residual collocation method that has no inherent numerical dissipation, and thus, there is no need to apply artificial dissipation to ensure numerical stability.

2 Methodology

2.1 Theory

Penetrative turbulence occurs when an unstably stratified large body of fluid underlies a stably stratified fluid layer. In this situation, turbulent eddies are driven vertically by the buoyancy force, and attempt to penetrate into the overlying stable fluid (Stull, 1976). In the stable region, when an eddy reaches its level of buoyancy, it returns back downward into the unstable region. However, due to the gained momentum, eddies often overshoot their level of buoyancy, and thus, internal waves are excited from the interface between the overlying stably stratified fluid and the underlying unstable mixing layer (Stull, 1976; Lane, 2008). These waves transports kinetic energy to the upper atmosphere, and may initiate upper level clear air turbulence. Deardorff et al. (1969)

investigated such penetrative turbulence experimentally. Here, we develop a large eddy simulation model to simulate the above mentioned phenomena.

2.2 Equations

For a compressible atmospheric model, the temperature (T) and the pressure (p) are represented by the potential temperature (θ) and the Exner function (π') (*e.g.*, Smolarkiewicz et al., 2014),

$$\theta = T \left(\frac{p_0}{p} \right)^{R_d/c_p}, \quad \pi' = \left(\frac{R_d}{p_0} \rho \theta \right)^{R_d/(c_p - R_d)},$$

respectively, where p_0 is a reference pressure, R_d is the gas constant, c_p is the specific heat at constant pressure, and ρ is the density. The continuity equation is replaced with Eq (1). The notation $(x_1, x_3) = (x, z)$ and $(u_1, u_3) = (u, w)$ are adopted for simplicity. A spatial filter is applied to the momentum and energy equations, where $u_i (\equiv \langle u_i \rangle)$ and $\theta (\equiv \langle \theta \rangle)$ represent filtered velocity and temperature, respectively. More specifically, $\tilde{u}_i = u_i + u'_i$ and $\tilde{\theta} = \theta_0 + \bar{\theta}(z) + \theta + \theta'$ (Deardorff, 1970, 1980). Note the separation of the reference temperature θ_0 from the background temperature $\bar{\theta}(z)$, which is convenient for satisfying the surface condition. The following equations are solved in the present work;

$$\frac{D\pi'}{Dt} = -\pi' \frac{\partial u_i}{\partial x_i}, \quad (1)$$

$$\frac{Du_i}{Dt} = -c_p \theta_0 \frac{\partial \pi'}{\partial x_i} + \frac{g\theta}{\theta_0} \delta_{i3} - \frac{\partial \tau_{ij}}{\partial x_j}, \quad (2)$$

$$\frac{D\theta}{Dt} = -w \frac{\partial \bar{\theta}}{\partial z} - \frac{\partial \tau_{\theta j}}{\partial x_j}. \quad (3)$$

The simulation region is a vertical plane (x, z) that extends 100 km horizontally ($-50 \leq x \leq 50$) and 2 km vertically ($0 \leq z \leq 2$). A city of scale 20 km exists for $-10 \leq x \leq 10$, which is surrounded by rural areas. Recent literature indicates that the most appropriate model for the near surface penetrative turbulence is not fully understood. As a compromise, as discussed by Pope (2000), we have adopted a resolution that is finer than that is used by LES models of the ABL. The finest resolution uses $\Delta x = 97.65$ m and $\Delta z = 3.9$ m. Thus, a significant fraction of the energy containing large eddies

is resolved. Here, some advantages of the costly three-dimensional simulation are sacrificed for a high resolution two-dimensional idealization (Lane, 2008).

2.3 Large eddy simulation

The subgrid scale turbulent stress is estimated by the popular Smagorinsky (1963) model, $\tau_{ij} = -2(C_s\Delta)^2|S|S_{ij}$, where $|S| = \sqrt{2S_{ij}S_{ij}}$ and $S_{ij} = (1/2)(\frac{\partial u_i}{\partial x_j} + \frac{\partial u_j}{\partial x_i})$. We define the filter width by $\Delta = \sqrt{\Delta x \cdot \Delta z}$, and take $C_s = 0.18$ for the Smagorinsky constant.

According to Deardorff (1980), the subgrid scale eddy coefficients may be computed by $K_h = (1 + 2l/\Delta)K_m$ and $K_m = 2(C_s\Delta)^2|S|$, where $l \leq \Delta$ is a subgrid scale mixing length. The length scale, l , is related to the subgrid scale turbulence energy e' and the buoyancy frequency, $N^2 = \frac{g}{\theta_0} \frac{\partial \theta}{\partial z}$, *i.e.* $l = 0.76\sqrt{e'}/N$. If the scale of resolved eddies is $\Delta = 20$ m, then a turbulent Prandtl number $Pr = 0.71$ gives $l \approx 4$ m. The SGS flux for buoyancy is $\tau_{\theta i} = -K_h \frac{\partial \theta}{\partial x_i}$ (Deardorff, 1980).

2.4 Surface heat-flux variation

We consider a time independent profile for the surface heat flux variation $H_{\text{sfc}}(x) = \langle H_{\text{sfc}} \rangle + H_0$ that is given by

$$H_{\text{sfc}}(x) = \langle H_{\text{sfc}} \rangle + A[\tanh \xi(x+\lambda/2) - \tanh \xi(x-\lambda/2)].$$

Here, $\langle H_{\text{sfc}} \rangle = 0.03 \text{ K m s}^{-1}$ (about 37 W m^{-2}) represents a domain average heat flux for all x in the range from -50 to 50 km, where there is no city induced heat flux H_0 . λ is the characteristic wavelength for the surface heat flux variation H_0 , where the heating region (city) of the surface is from -10 to 10 km, *i.e.* $\lambda = 20$ km. This choice for λ represents the resolved scale for mesoscale numerical weather prediction models. $\xi = 100$ is a dimensionless number that leads to a continuous sharp interface between the central heating region and other part of the surface. Thus, the surface heat flux $H_{\text{sfc}}(x)$ takes approximately the form of a square wave without sharp corners, and models the effect of urban-rural heat flux variation. This article summarizes the sensitivity of surface heat flux on penetrative

turbulence for 6 values of H_0 . A purpose of these simulations is to understand the sensitivity of high-amplitude surface heat-flux heterogeneity for temporal oscillation in mesoscale atmospheric circulations.

2.5 Validation

The total heat flux is composed of turbulent ($\overline{w'\theta'}$) and viscous ($\alpha \frac{\partial \theta}{\partial z}$) components, where the turbulent component vanishes on a flat surface. The dimensionless surface heat flux takes the form $-\frac{1}{\sqrt{RaPr}} \frac{\partial \theta}{\partial z}|_{z=0}$, where the potential temperature is the same the surface temperature.

A scale analysis is necessary to compare the present model with that presented by Dubois and Touzani (2009). With a fully developed turbulence in the convective boundary layer, the vertical temperature profile satisfies $\frac{\partial \theta}{\partial z} = 0$ in mixing region ($z > 0$) (Deardorff et al., 1969). In this case, natural convection heat transfer is characterized by the Rayleigh number $Ra = \frac{gH^3}{\theta_0\nu\kappa} \frac{H_0H}{\alpha}$, where H is a vertical length scale, $1/\theta_0$ is the coefficient of thermal expansion (1/K), ν is the kinematic viscosity (m^2/s), κ is thermal conductivity ($\text{W/m}\cdot\text{K}$), g is the acceleration due to gravity (m/s^2), and α is the thermal diffusivity (m^2/s). In an LES, ν and α can be replaced with K_m and K_h , respectively. So, we set $\frac{H_0H}{\alpha} = 10^\circ\text{K}$ to match the adiabatic lapse rate (10°K/km) of the atmosphere so that $\frac{\partial \theta}{\partial z} = 0$. As a result, an increase of H_0 by a factor of 2 increases Ra by a factor of 10. Thus, the values of $H_0 = 57.87 \text{ W m}^{-2}$ and 115.74 W m^{-2} represents $Ra = 10^4$ and 10^5 , respectively. The comparison is summarized in Table 1. In addition, we have compared the vertical profile of mean temperature with that obtained from the Wangara day 33 experiment, which shows an excellent agreement on $\frac{\partial \theta}{\partial z} = 0$ between two data sets.

3 Results

3.1 Surface induced impact of air pollution

Fig 1(a) demonstrates an example of surface induced impact on air pollution. The turbulent plume from the lower chimney (75 m tall) moves toward the region of

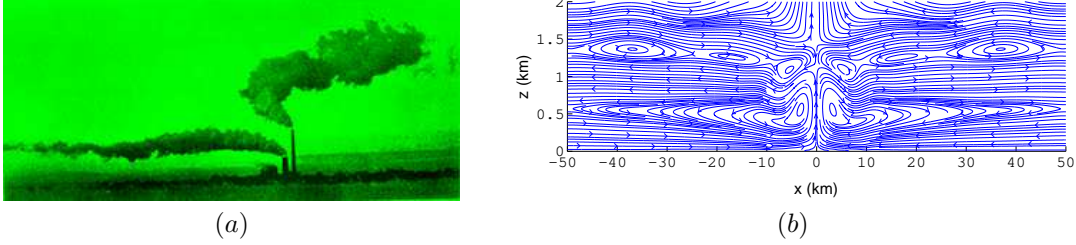


Figure 1: (a) Movement of plumes from two chimneys of unequal height as a result of differential surface heating. The figure is adapted from Google image database, and represents a pattern of expected circulation. (b) Low level converging flow and high level diverging flow is seen from this streamline at $t = 6.5$ h for $H_0 = 115.74 \text{ W m}^{-2}$.

warmer surface (city area), and that from the higher chimney (150 m tall) moves toward the region of cooler surface (urban, ocean). The atmosphere over the warmer surface has a decreased thermal stability, which causes a low level converging flow. Thus, the air parcels move horizontally toward the center of the heated region, where they rise upward. The characteristic flow pattern in Fig 1 is observed from our numerical simulation. The comparison in Fig 1 indicates that our numerical model simulates phenomena that is also observed in the nature. The streamline plot in Fig 1(b) shows that air moves to the left in the lower portion of the boundary layer above $x > 0$, and the air in the upper portion moves to the right. This flow pattern is computed at $t = 6.5$ h from the simulation with $H_0 = 231.48 \text{ W m}^{-2}$.

3.2 Turbulent mixed layer formation

To understand the mixing and turbulent transport in the absence of shear or mechanically driven turbulence, we have initialized the flow with a stable stratification

H_0	57.87 W m^{-2}		115.74 W m^{-2}	
	Present	D & T	Present	D & T
θ_{\min}	-0.0644	-0.0712	-0.1672	-0.1663
u_{\max}	0.1761	0.1748	0.1796	0.1790
w_{\max}	0.2275	0.2282	0.3294	0.3224
Nu	0.3262	0.2951	0.6892	0.6435

Table 1: Comparison of dimensionless extreme values with that from Dubois and Touzani (2009) (D & T).

and no background wind everywhere except an unstable stratification is introduced near the surface. The surface Richardson number $Ri_0 = (\frac{g}{\theta_0} \frac{\partial \theta}{\partial z}|_{z=0}) H^2 / U^2$ controls the initial strength of unstable stratification. The flow is initialized with $Ri_0 = -1$, and allowed to evolve naturally with time. Thus, the resulting circulations characterize penetrative turbulent convection (Deardorff et al., 1969). The time evolution of the streamlines in the entire domain is shown in Fig 2.

The relative surface heat flux for $-10 \leq x \leq 10$ is $H_0 = 925.92 \text{ W m}^{-2}$ ($\sim 0.75 \text{ K m s}^{-1}$), where the background potential temperature $\bar{\theta}(z)$ in the stable region has a gradient $10^\circ/1 \text{ km}$, and the buoyancy frequency is $N \approx 10^{-2} \text{ s}^{-1}$. As seen from Fig 2, when the sun heats the surface, eddies begin to form and rise upward. However, they return back downward due to stable stratification in the upper atmosphere. This generates an unstable mixing layer that is adjacent to the surface. This turbulent mixed layer underlies a stable region aloft. Based on the mean vertical profile of potential temperature (not shown), the depth of the mixed layer for this simulation is approximately 800 m.

When an eddy loses buoyancy, it rises upward, and a negative horizontal buoyancy gradient occurs near its left edge, which generates a cyclonic circulation; similarly, anticyclonic circulation is formed on the other edge of the eddy (Lane, 2008; Alam, 2011). The pattern of such a circulation and the time evolution of the associated span-wise vorticity, during a penetrative turbulent convection, is realized from the streamlines in Fig 2. This vortical pattern play its role as a heat transfer agent, thereby causing a imbalance between the buoy-

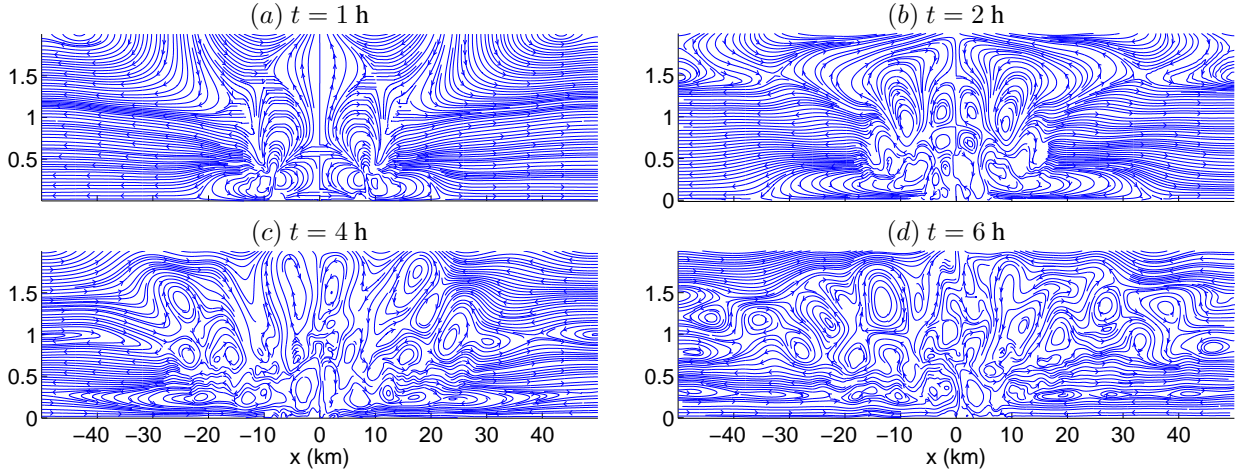


Figure 2: The time evolution of span-wise vorticity is demonstrated using the streamline at $t = 1$ h, $t = 2$ h, $t = 4$ h, and $t = 6$ h for the simulation with $H_0 = 925.92 \text{ W m}^{-2}$.

ancy force and gravitational force. An important question of meteorological interest is whether the process leads to horizontal turbulent fluctuation, and if such fluctuation affects local weather prediction. At $t = 1$ h, cyclonic/anticyclonic eddies have been formed near the outer edges of the heating region, and have reached a height of about 500 m. Later, horizontal convection is observed; *i.e.* turbulent eddies move horizontally, where turbulent eddies reach a maximum vertical height of about 800 m. Entrainment/detrainment occurs above this height.

3.3 Temporal oscillation and downscale energy cascade

According to the Taylor's hypothesis, if turbulent statistics is approximately stationary and homogeneous, then the turbulent field is advected over the time scales of interest. Under this hypothesis, time series of potential temperature and horizontal velocity, as shown in Fig 3, indicate that surface heterogeneity on a scale $\mathcal{O}(20 \text{ km})$ contributes toward downscale energy cascade. The growth of the horizontal potential temperature gradient develops a horizontal pressure gradient, which in turn generates horizontal wind. The time series of θ and u at several vertical locations have been analyzed to

characterize penetrative turbulence.

The sensitivity of surface heat flux on the temporal fluctuation of θ is clear from Fig 3. At $z = 62.5$ m, frequency of oscillation increased at $H_0 = 925.92 \text{ W m}^{-2}$ compared to $H_0 = 462.96 \text{ W m}^{-2}$. However, at $z = 500$ m, turbulence is seen fully developed in both cases. This indicates that turbulent kinetic energy cascades downscale as the energy is transported by internal waves. To verify that air flow over the simulated city is characterized by a horizontal flow of numerous rotating eddies, we present the horizontal velocity u , which is the wind component that is parallel to the direction of the surface heat flux variation. The onset of turbulent fluctuations is compared between two surfaces fluxes in Fig 4.

4 Concluding remarks

In this article, we report some aspects of penetrative turbulence in an idealized daytime boundary layer over a city that is surrounded by rural areas. As internal waves excite from the interface between the mixed layer and stable layer, kinetic energy of boundary layer turbulence is transferred to upper label free atmosphere. A complete understanding of this mechanism remains

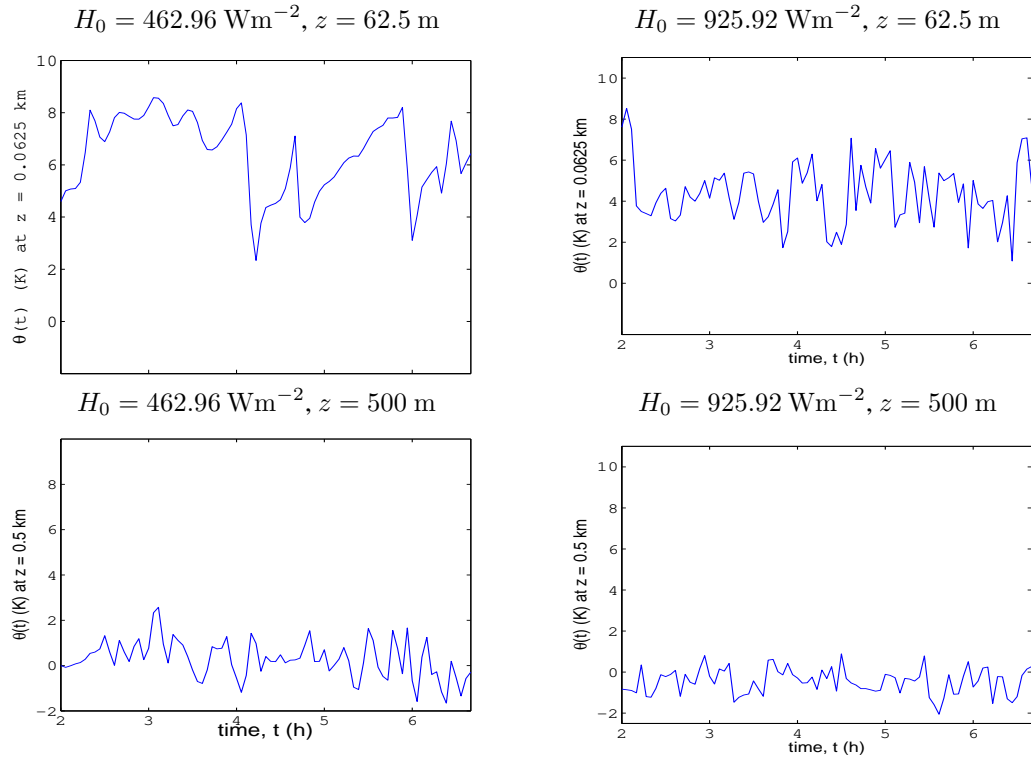


Figure 3: Time series of potential temperature $\theta(0, z, t)$ near the surface ($z = 62.5 \text{ m}$) and near top of the mixing layer ($z = 500 \text{ m}$).

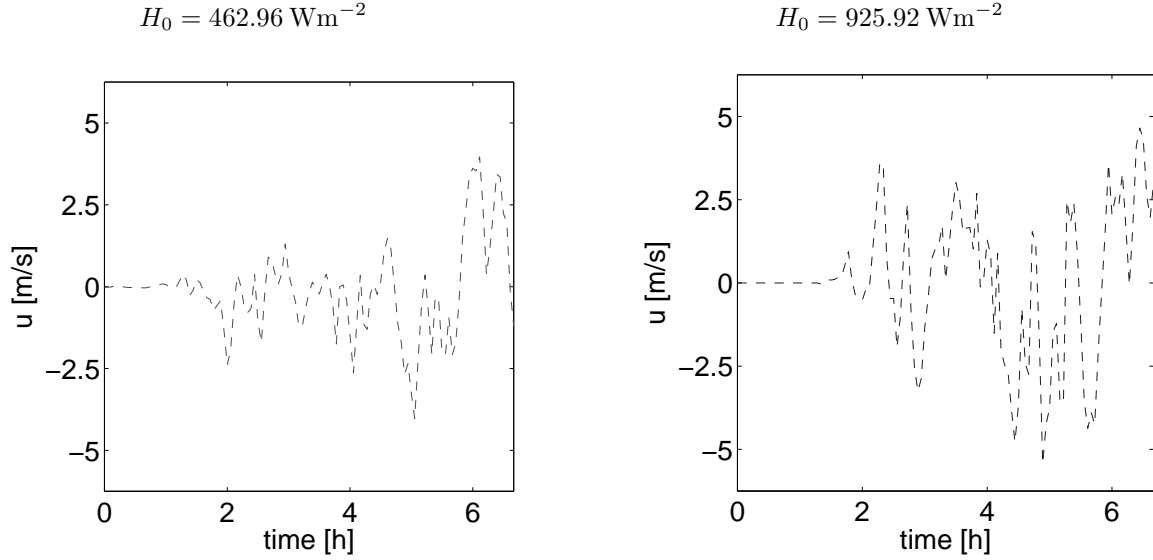


Figure 4: The onset of turbulent fluctuation is shown through time series of horizontal velocity at $z = 100$ m from the surface.

a challenging future research topic. However, in the present article, we have shown that energy cascades downscale as turbulence penetrates upward. Our simulations demonstrate that characteristics of the induced horizontal flow may be significantly different depending on the surface heterogeneity from the perspective of the turbulence that is generated.

The simulation is idealized. However, we have studied characteristics of horizontal flow with surface heat-flux variation on the scale of 20 km, which is the typical grid spacing in numerical weather prediction models. One of our objectives is to understand if thermally induced mesoscale perturbation has a connection to penetrative turbulence. In other words, we show that differential heating on the same label leads to a sustained turbulent flow. Note that we have compromised the three-dimensional simulation with a two-dimensional one in order to capture the energy containing large eddies. These results suggest that surface heterogeneity induced differential heating causes subgrid scale turbulent fluctuations, and the impact of surface heterogeneity could be more substantial on mesoscale atmospheric flows. In future studies, we plan to continue fully three-dimensional LES of penetrative turbulence. We plan to

investigate how temporal oscillations characterize turbulent energy cascade, particularly with background wind conditions and rough surface.

References

- Alam, J. (2011). Towards a multi-scale approach for computational atmospheric modelling. *Monthly Weather Review*, 139(12).
- Alam, J. M., Walsh, R. P., Alamgir Hossain, M., and Rose, A. M. (2014). A computational methodology for two-dimensional fluid flows. *International Journal for Numerical Methods in Fluids*, 75(12):835–859.
- Bryan, G. H. and Fritsch, J. M. (2002). A benchmark simulation for moist nonhydrostatic numerical model. *Mon. Wea. Rev.*, 130.
- Deardorff, J. (1980). Stratocumulus-capped mixed layers derived from a three-dimensional model. *Boundary-Layer Meteorology*, 18(4):495–527.

- Deardorff, J. W. (1970). A three-dimensional numerical investigation of idealized planetary boundary layer. *Geophys. Fluid Dyn.*, 1:377–410.
- Deardorff, J. W., Willis, G. E., and Lilly, D. K. (1969). Laboratory investigation of non-steady penetrative convection. *Journal of Fluid Mechanics*, 35.
- Dubois, T. and Touzani, R. (2009). A numerical study of heat island flows: Stationary solutions. *International Journal for Numerical Methods in Fluids*, 59(6):631–655.
- Lane, T. P. (2008). The vortical response to penetrative convection and the associated gravity-wave generation. *Atmos. Sci. Lett.*, 9:103–110.
- Lin, Y.-L. (2007). *MESOSCALE DYNAMICS*. Cambridge University Press.
- Paparella, F. and Young, W. R. (2002). Horizontal convection is non-turbulent. *Journal of Fluid Mechanics*, 466:205–214.
- Pope, S. B. (2000). *Turbulent Flows*. Cambridge University Press.
- Sandström, J. W. (1908). Dynamische versuche mit meerwasser. *Annalen der Hydrographie und Maritimen Meteorologie*, 36:6–23.
- Scotti, A. and White, B. (2011). Is horizontal convection really non-turbulent?. *Geophysical Research Letters*, 38(21).
- Skamarock, W. C. and Klemp, J. B. (2008). A time-split nonhydrostatic atmospheric model for weather research and forecasting applications. *J. Comput. Phys.*, 227(7):3465–3485.
- Smolarkiewicz, P. K., Kühnlein, C., and Wedi, N. P. (2014). A consistent framework for discrete integrations of soundproof and compressible pdes of atmospheric dynamics. *J. Comput. Phys.*, 263:185–205.
- Stull, R. B. (1976). Internal gravity waves generated by penetrative convection. *J of the Atmospheric Sciences*, pages 1279–1286.